ONIOM Study of Chemical Reactions in Microsolvation Clusters: $(H_2O)_nCH_3Cl + OH^-(H_2O)_m$ ($n + m = 1$ and 2)

Suyong Re[†,‡] and Keiji Morokuma*[,‡]

Department of Chemistry, Faculty of Science, Rikkyo University, 3-34-1 Nishi-ikebukuro, Toshima-ku, Tokyo 171-8501, Japan, and Cherry Emerson Center for Scientific Computation and Department of Chemistry, Emory University, Atlanta, Georgia 30322

Received: December 31, 2000; In Final Form: May 7, 2001

The reliability of the two-layered ONIOM (our own N-layered molecular orbital + molecular mechanics) method was examined for the investigation of the S_N2 reaction pathway (reactants, reactant complexes, transition states, product complexes, and products) between CH_3Cl and an OH^- ion in microsolvation clusters with one or two water molecules. Only the solute part, CH_3Cl and OH^-, was treated at a high level of molecular orbital (MO) theory, and all solvent water molecules were treated at a low MO level. The ONIOM calculation at the MP2 (Møller−Plesset second order perturbation)/aug-cc-pVDZ (augmented correlation-consistent polarized valence double-ζ basis set) level of theory as the high level coupled with the B3LYP (Becke 3 parameter-Lee-Yag-Parr)/6-31+G(d) as the low level was found to reasonably reproduce the "target" geometries at the MP2/aug-cc-pVDZ level of theory. The energetics can be further improved to an average absolute error of <1.0 kcal/mol per solvent water molecule relative to the target CCSD(T) (coupled cluster singles and doubles with triples by perturbation)/aug-cc-pVDZ level by using the ONIOM method in which the high level was CCSD(T)/aug-cc-pVDZ level with the low level of MP2/aug-cc-pVDZ. The present results indicate that the ONIOM method would be a powerful tool for obtaining reliable geometries and energetics for chemical reactions in larger microsolvated clusters with a fraction of cost of the full high level calculation, when an appropriate combination of high and low level methods is used. The importance of a careful test is emphasized.

I. Introduction

Chlorinated hydrocarbons (CHCs) have been used as a solvent and a degreaser in a range of industrial applications for a long time, and the used solvent was, unfortunately, simply dumped into landfills, exposed ditches, and drains. Consequently CHCs are recently becoming the most ubiquitous contaminant on earth as a whole, and it is thus obviously required to clarify the fate of such contaminants in nature. CHCs are known to be degradable by abiotic processes such as hydrolysis. The investigation of their behavior in groundwater, such as reactions with OH^-, metal ions, and others, is considered to be very important.

Although there have already been some studies (both theoretical[1−5] and experimental[6−11] about the hydration process of CHCs and their reaction with OH^-, the overall picture for possible reaction pathways has not be fully understood. To explore the potential energy surface for the reaction in water solvent, a difficult but important problem is how to evaluate the profound effect of water solvent on reaction mechanism. Although recent theoretical techniques enable us to calculate the solute electronic structure under the effect of water solvent by using those such as the polarized continuum model,[12,13] it would be a better way, if possible, to explicitly treat at least the first solvent shell of water molecules using the microsolvated cluster.

A first theoretical study for the reaction of methyl chloride with hydroxy anion in a microsolvated cluster

$$(H_2O)_nOH^- + CH_3Cl(H_2O)_m \rightarrow (H_2O)_{n'}HOCH_3 + Cl^-(H_2O)_{m'} \quad (1)$$

was performed for the reaction $CH_3Cl + OH^-$ by Ohta et al. with one and two water solvent molecules ($n + m = n' + m' = 1$ and 2) at the ab initio HF level of the MO method.[1] Subsequent studies suggested that the quantitative description of the S_N2 reaction requires a high level of correlation treatment with a large basis set.[14] A very high level study of the reaction $CH_3Cl + OH^-$ with one and two water molecules has recently been performed by Garrett et al.[15] They found that CCSD(T)/aug-cc-pVDZ single-point energy at the geometry optimized at the MP2/aug-cc-pVDZ level gives nearly quantitatively correct results for ($n + m = n' + m' = 1$ and 2). However, this level of calculation requires an extremely large amount of supercomputer time, and calculations for the same reaction system with three or more water molecules would be very difficult even with the maximum use of the supercomputer time.

The recently developed ONIOM (Our own N-layered integrated molecular orbital + molecular mechanics) method provides a possibility to achieve such high accuracy calculation on a large molecular system. In the two-layer MO + MO version of ONIOM,[16] also called IMOMO (integrated MO + MO),[17] the active part of the reaction is considered in the "model" system and is treated with both at "high" and "low" levels of MO calculation, whereas the entire "real" system is treated only

* To whom correspondence should be addressed. E-mail: morokuma@emory.edu.
† Rikkyo University.
‡ Emory University.

10.1021/jp004623a CCC: $20.00
Published on Web 07/07/2001

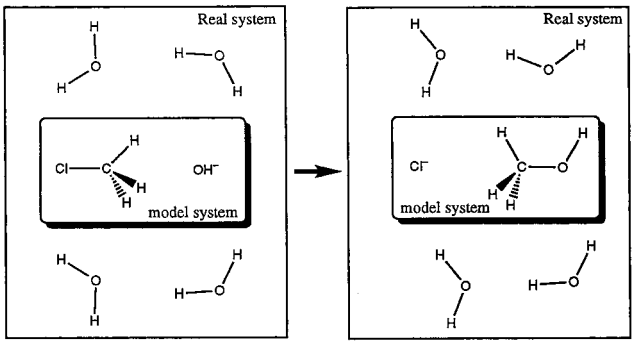

Figure 1. Scheme of the real and model system used in the ONIOM calculations for reaction $CH_3Cl + OH^-$ in hydrated clusters.

at the "low" level of MO calculation, and then they are integrated to define the ONIOM total energy of the "real" system.

$$E(\text{ONIOM, real}) = E(\text{high, model}) + E(\text{low, real}) - E(\text{low, model}) \quad (2)$$

The ONIOM energy is an extrapolation or additive approximation for the "target" calculation, *E*(high, real), the "high" level calculation for the "real" system, which is too expensive to perform. The definition of the "model" system and the choice of the levels of calculation are left to the users and depend on the errors that can be tolerated in the ONIOM treatment. It should be recognized that a careless choice of level combination in the ONIOM method leads to a failure, and a careful test of the reliability of a given level combination has to be made. The clearly defined requirement of the "low" level method is that it reproduces reliably the substituent effect, i.e., the difference between the real system and the model system, calculated at the "high" level.

The ONIOM method has already been applied to the studies of the steric effect for the S_N2 reaction between Cl^- and alkyl chloride and has been found to give a very good approximation for "high" level geometry and energetics including the barrier.[17] The aim in the present series of studies is to obtain as accurate results as possible for large hydrated cluster systems using the ONIOM method, in which all of the solvent water molecules are treated only at the low level. If this could be done, we are ready to investigate the reaction mechanism of highly hydrated ($m + n > 3$) CHCs with the OH^- ion.

In the present study, we will compare geometries of intermediates and transition states (TSs) of the reaction 1 for $n + m = n' + m' = 1$ and 2 optimized at various ONIOM combinations with those optimized at the target MP2 level and assess what low level is needed. We will perform a similar energetic comparison between the high level pure MO method and the ONIOM methods to examine the low level needed for accurate description potential energy profiles.

II. Method of Calculation

The detail description for the ONIOM method has already been published elsewhere.[17] The accuracy of the ONIOM method depends much on the choice of the model system and the low level of the method. In the present ONIOM calculations, the model system consists of only CH_3Cl and the OH^- ion, which will be treated with both the high and the low level of method. All of the surrounding water molecules are included in the real system, which is calculated only at the low level method as shown in Figure 1.

Very accurate results of equilibrium and transition state geometries and their energies obtained at the CCSD(T)/aug-cc-pVDZ//MP2/aug-cc-pVDZ level of theory, i.e., the single-point calculation at the CCSD(T)/aug-cc-pVDZ (hereafter referred to as CC/b) level at the optimized geometries at the frozen core MP2/aug-cc-pVDZ (referred to as MP2/b) level, for reaction 1 with for $n + m = n' + m' = 1$ and 2 have been provided to us by Garrett and Borisov.[15] Because not all of the stationary points were available, we also performed additional calculations at the same level to supplement their results. We will use these results as the "target" calculations of the ONIOM studies; namely, we will compare the ONIOM geometries and energies with these "target" results to assess the errors associated with the ONIOM extrapolation scheme. We will naturally choose the level used in the pure MO calculation as the "high" level of the ONIOM method.

For geometry optimization, we examined three types of methods as the "low" level. Recent reports show that gradient-corrected and hybrid DFT methods provide reasonable results with relatively lower cost for some of hydrogen-bonded cluster system.[18−23] We, therefore, employed density functional gradient-corrected BLYP and hybrid B3LYP methods[24−26] as well as the HF method as the low level. In all low level calculations, we used the 6-31+G(d) basis set, a smallest basis set required to describe hydrogen-bonding anionic systems (referred to as BLYP, B3LYP, and HF), The notation like "(MP2/b:HF)" is used to indicate the "high level:low level" combination in the ONIOM method. The ONIOM geometries are, then, compared with the "target" geometries at the MP2/aug-cc-pVDZ level.

To improve the accuracy of energetics, single-point energy calculations are performed on the above ONIOM optimized geometries by using another ONIOM combination, where the CC/b method is used as the "high" level and MP2/6-31+G(d) (referred to as MP2), B3LYP, and BLYP methods are employed as the "low" level. The obtained energetics will be compared with the target CC/b//MP2/b level of results. All of the calculations were performed by using Gaussian 98[27] and a development version of the Gaussian package.

III. Results and Discussions

According to previous theoretical studies,[1] the S_N2 reaction between microsolvated $(H_2O)_nOH^-$ with $CH_3Cl(H_2O)_m$ for $m + n = 1$ and 2 proceeds through a prereaction complex and the transition state, followed by highly exothermic energy release process involving the migration of water molecules to give product complexes. The potential energy profiles calculated at the CC/b//MP2/b level, by Borisov and Garrett[15] and supplemented by us, are summarized in the Figure 2. Here **RC0**, **RC1**, and **RC2** are the prereaction complexes $(H_2O)_nOH^-\cdots CH_3Cl(H_2O)_m$, **TS0**, **TS1**, and **TS2** are the transition states and **PC0**, **PC1**, and **PC2** are the product complexes $(H_2O)_{n'}HOCH_3\cdots Cl^-(H_2O)_{m'}$ for $m + n = m' + n' = 0$, 1, and 2, respectively. The MP2/b optimized geometries ("target" geometries) are shown in Figures 3−8. Because the purpose of the present paper is not exploring overall potential energy surfaces but examining the reliability of the ONIOM method for this system, only the reaction pathway described above would be considered.

In the present ONIOM study where solvent molecules are treated at the low level, the requirement for the low level in the ONIOM method is to reasonably describe the solute−solvent as well as solvent−solvent interactions in comparison with the target calculation. In the following discussion, we will pay our attention to how various low levels of pure MO methods as well as various ONIOM combinations reproduce the benchmark results and seek the most suitable method as a low level in the ONIOM method.

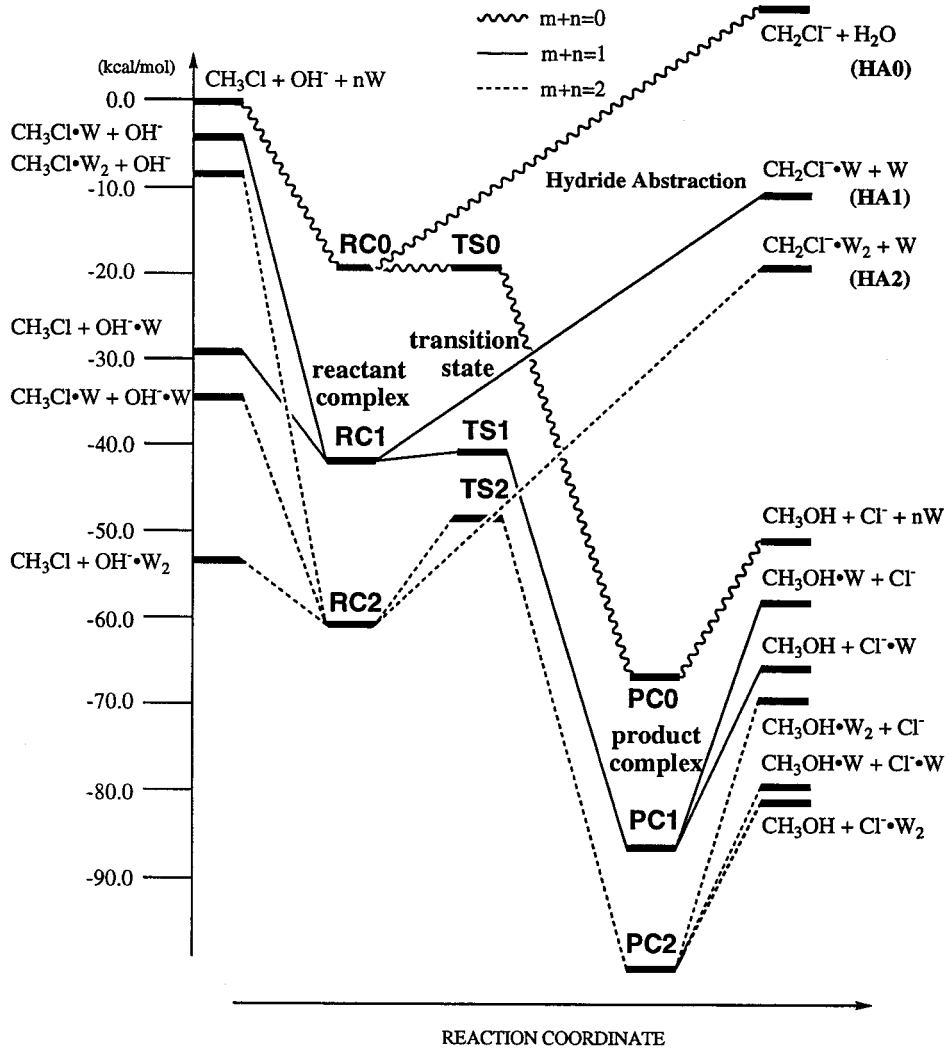

Figure 2. CCSD(T)/aug-cc-pVDZ//MP2/aug-cc-pVDZ (CC/b//MP2/b) potential energy profiles for reaction, $W_nOH^- + CH_3ClW_m$ ($n + m = 1$ and 2), where W denotes H_2O. Here **RC0**, **RC1**, and **RC2** are the prereaction complexes $(H_2O)_nOH^- + CH_3Cl(H_2O)_m$, **TS0**, **TS1**, and **TS2** are the transition states, and **PC0**, **PC1**, and **PC2** are the product complexes $(H_2O)_{n'}HOCH_3 + Cl^-(H_2O)_{m'}$ for $m + n = m' + n' = 0$, 1, and 2, respectively.

A. MO and ONIOM Optimized Geometries. *HF and DFT vs "Target" (MP2/b) Optimized Geometries.* To seek the best candidate for the lower level method in the ONIOM calculation, we first examine the geometries obtained with three types of the pure MO method (B3LYP, BLYP, and HF) and compared with the "target" (MP2/b) geometries. All of the geometries obtained at the pure MO methods are shown in left column of the figures. Optimized geometries of reactant molecules and their hydrated clusters determined at the "target" level are shown in Figure 3 together with those at the lower level of pure MO methods. The structures of $X^-(H_2O)_n$ (X = OH and Cl) at the "target" level of method are in good agreement with the previously reported results.[28−31] In contrast, we could not obtain the structure reported previously[1] for the $CH_3Cl(H_2O)$ complex with the water molecule interacting only with chlorine atom. Because this geometry optimization was performed under the C_s symmetry assumption, the present result without such assumption would be more reliable. Three lower levels of the pure MO methods (HF, BLYP, and B3LYP) provide similar results as those obtained with the "target" calculation. In particular, the B3LYP method well describes the hydrogen-bond distances with less than 0.1 Å of differences from the benchmark values, in contrast to 0.1∼0.3 Å differences at the HF level.

Optimized structures of the reactant complexes are shown in Figure 4. In the $n + m = 0$ structure at the MP2/b level,[15] OH^- coordinates to one of the hydrogen atoms of the methyl group. For the $n + m = 1$ system (**RC1**), all pure MO methods provide similar geometries, where $OH^-(H_2O)$ coordinates to CH_3Cl to form two hydrogen bonds between them. Note that the OH^- ion is more strongly attracted toward the carbon atom of methyl chloride at the BLYP level compared to the other methods, resulting in shorter $C\cdots OH^-$ and longer $ClCH_3\cdots OH_2$ distances as well as a larger ∠C−OH−HOH angle than that for MP2/b.

For the dihydrated system ($n + m = 2$), the "target" calculation provides the multiring structure, where the $OH^-(H_2O)_2$ fragment, forming a cyclic hydrogen-bond ring, interacts via three oxygen atoms with three hydrogen atoms of CH_3Cl. Although the structure is highly strained, the net-stabilization owing to the multiring of hydrogen bonding would stabilize the complex (**RC2**). It should be mentioned that this highly networked structure (**RC2**) is, however, not reproduced with any other pure MO method; the optimizations lead to the singly hydrogen-bonded structure between CH_3Cl and $OH^-(H_2O)_2$ (**RC2′**).

Figure 5 depicts the optimized geometries of the transition state for the substitution reaction with CH_3 inversion in both bare ($n + m = 0$) and hydrated ($n + m = 1$ and 2) systems. Note that the transition state for the bare system (**TS0**) could not be obtained with full density functional methods. For the monohydrated system, we obtained the structure (**TS1**) at all

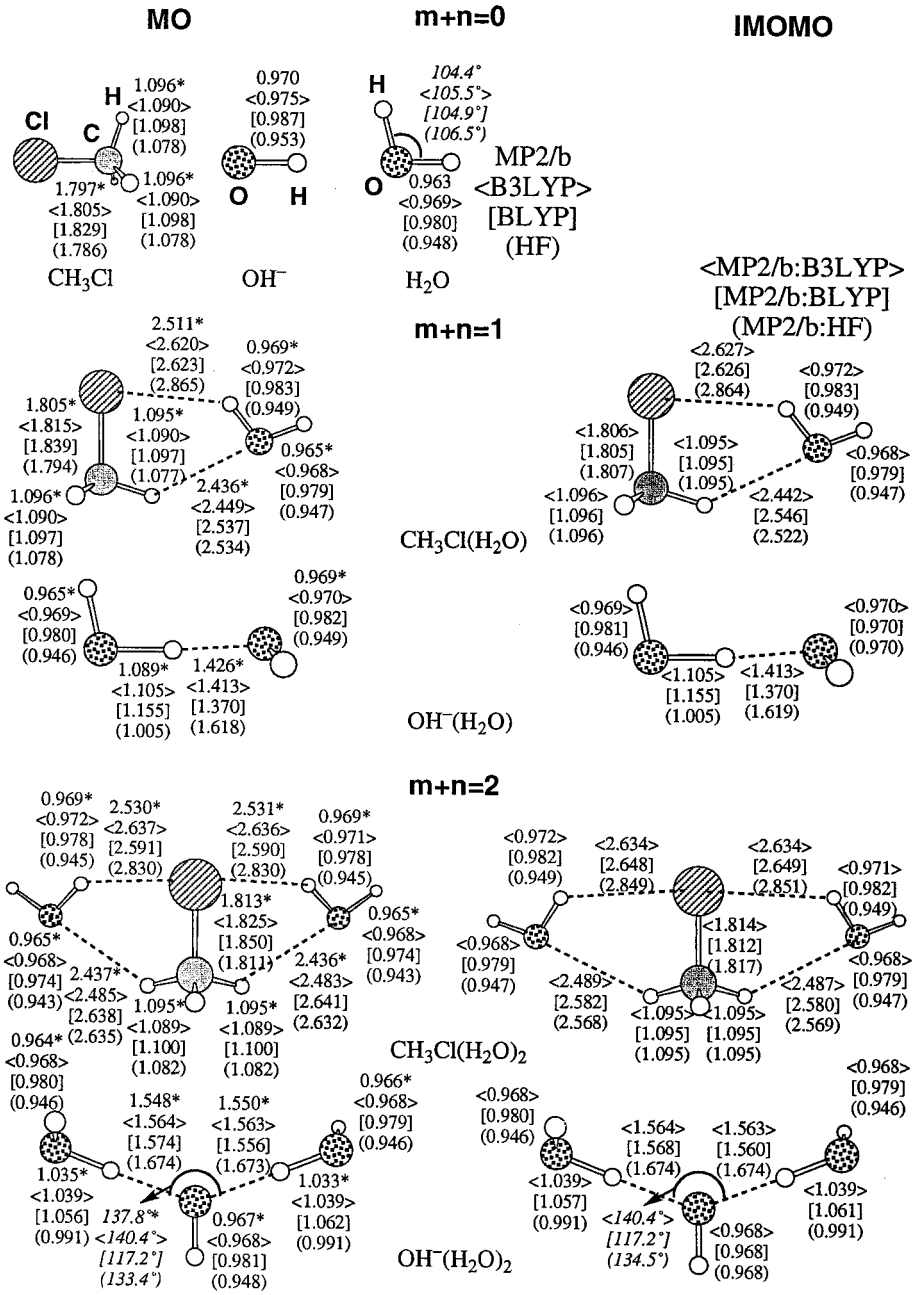

Figure 3. MO and ONIOM optimized geometries (in Å and deg) of reactant species for reaction 1 for $m + n = m' + n' = 0$, 1, and 2, respectively. For pure MO methods, geometrical parameters from the top are at the level of MP2/b (target), B3LYP (in <>), BLYP (in []), and HF (in ()), and for the ONIOM methods, the high level is MP2/b and the low level is B3LPY (in <>), BLPY (in []), and HF (in ()), respectively. For the target calculation, an asterisk indicates the value from ref 15 and without an asterisk indicates the value obtained by us.

of the MO levels, where H_2O molecule bounds on OH^-. In any level, we could not obtain the other TS reported previously with C_s symmetry constraint,[1] in which H_2O molecule is bounded on the Cl^- side. Because the interaction with H_2O is much weaker for Cl^- than for OH^-, such a structure could be a shallow potential energy minimum under symmetry restriction and may not exist as a real local minimum. In the **TS1** structure at the MP2/b level, Cl−C and C−O distances are calculated to be 0.07 Å longer and 0.104 Å shorter than those in the bare ($n + m = 0$) system. The three other pure MO methods provide similar qualitative structures, whereas the C−O bond length is longer by 0.1∼0.3 Å and the ∠C−O−H angle is much larger than that of the MP2/b values.

In the case of the $m + n = 2$ cluster system, a significant discrepancy is found for the results between the "target" and the other pure MO methods. There may exist logically the several TSs for the S_N2 reaction. Two most probable TSs are obtained with the "target" (MP2/b) method. One, denoted as **TS2c**, is the transition state, where two H_2O molecules are moving from OH^- to Cl^- concertedly with the substitution/CH_3 inversion. This structure is similar to the transition state for the substitution/CH_3 inversion for $Cl^- + CH_3Cl + 2H_2O$, found by Asada et al.[32] The other is one denoted as **TS2s**, where two H_2O molecules are unmoved and stay on OH^-. Note that we could not find the TS with one or two H_2O molecules on Cl^- because of the same reason as discussed for $m + n = 1$. The Cl−C and Cl−O bond distances in **TS2c** are 0.084 Å longer and 0.132 Å shorter at MP2/b level, respectively, than those in the bare ($n + m = 0$) system. The corresponding values for **TS2s** are 0.129 and 0.182 Å, respectively. The latter is thus a much later transition state than the former. Three other pure MO methods gave essentially the same structure for **TS2s** but

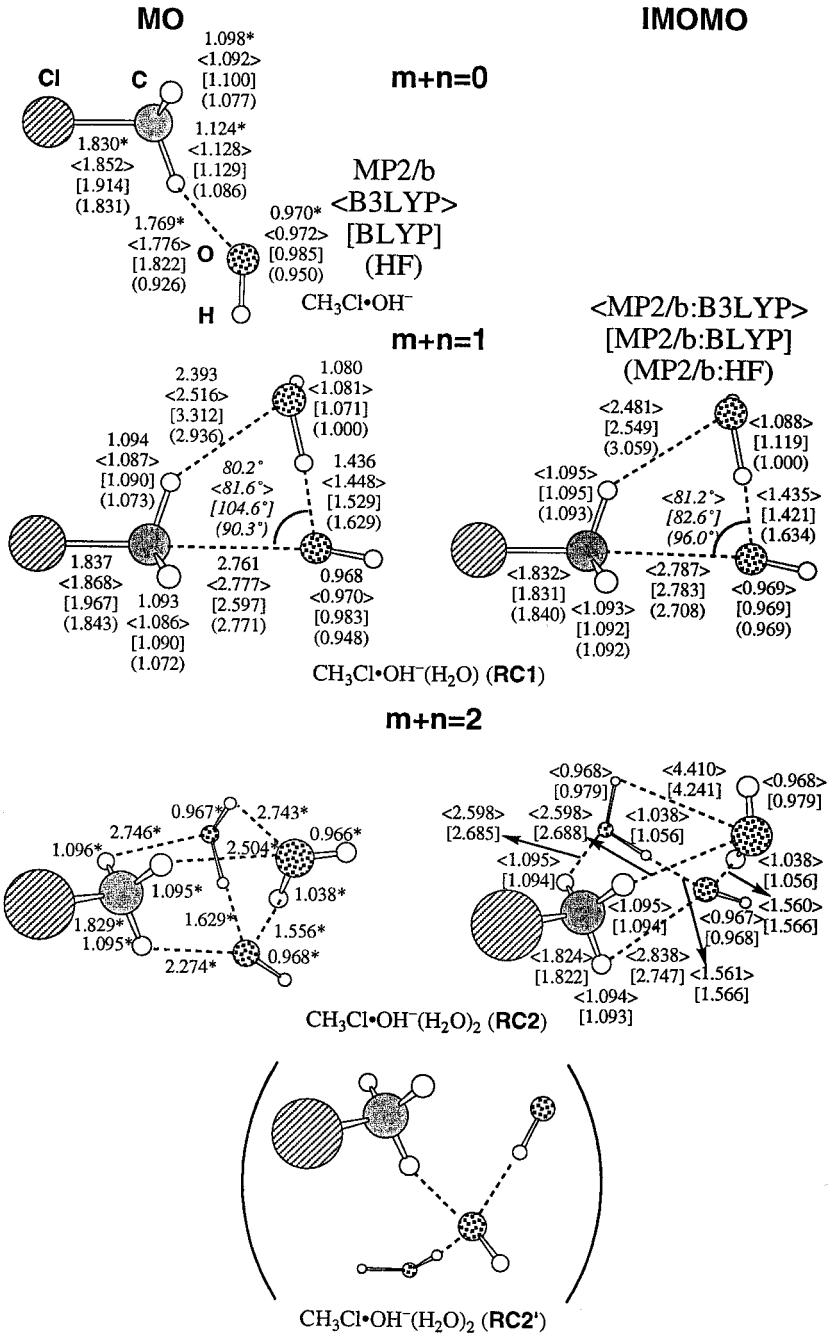

Figure 4. MO and ONIOM optimized geometries (in Å and deg) of reactant complexes for reaction 1 for $m + n = m' + n' = 0$, 1, and 2. For methods used, see Figure 3.

for **TS2c**. The **TS2c** structure is completely missed at the HF level; the optimization converged to **TS2s**. In addition, the nature of **TS2c** is qualitatively different between the DFT and the "target" level. The Cl−C distance in the **TS2c** structure is shorter than the C−O distance at the BLYP level, and they are identical at the B3LYP level, whereas at the target MP2/b level, Cl−C is longer than C−O. Compared with the "target" level, the DFT methods seem to unable to describe the nature of the charge transfer state, although it can describe the concerted feature of the TS; the HF method fails in both aspects.

Figure 6 illustrates the product complexes for the monohydrated (**PC1**) and dihydrated (**PC2**) systems. Both of the HF and the DFT methods reasonably reproduce the "target" geometries. The optimized structures for the product species (Figure 7) obtained at the low level of MO methods are all in reasonable agreement with the "target" geometries.

In Figure 8, we additionally show the optimized structures of the products of the hydride abstraction channel:

$$(H_2O)_nOH^- + CH_3Cl(H_2O)_m \rightarrow (H_2O)_{n'+1} + (CH_2Cl^-)(H_2O)_{m'} \quad (3)$$

This reaction was found to be highly endothermic, and the path is in essence simply uphill or has a small reverse barrier from the product complex. For instance, for the $m + n = 0$ system, target MP2/b optimization gives a TS with the energies of RC, TS, PC, and products (relative to the reactants) of −16.4, −10.8, −10.9, and 11.0 kcal/mol, respectively. The MP2 and HF methods respectively give a similar hump, whereas the DFT method gives no hump. For the monohydrated system, pure B3LYP and HF calculations give similar structures to that of

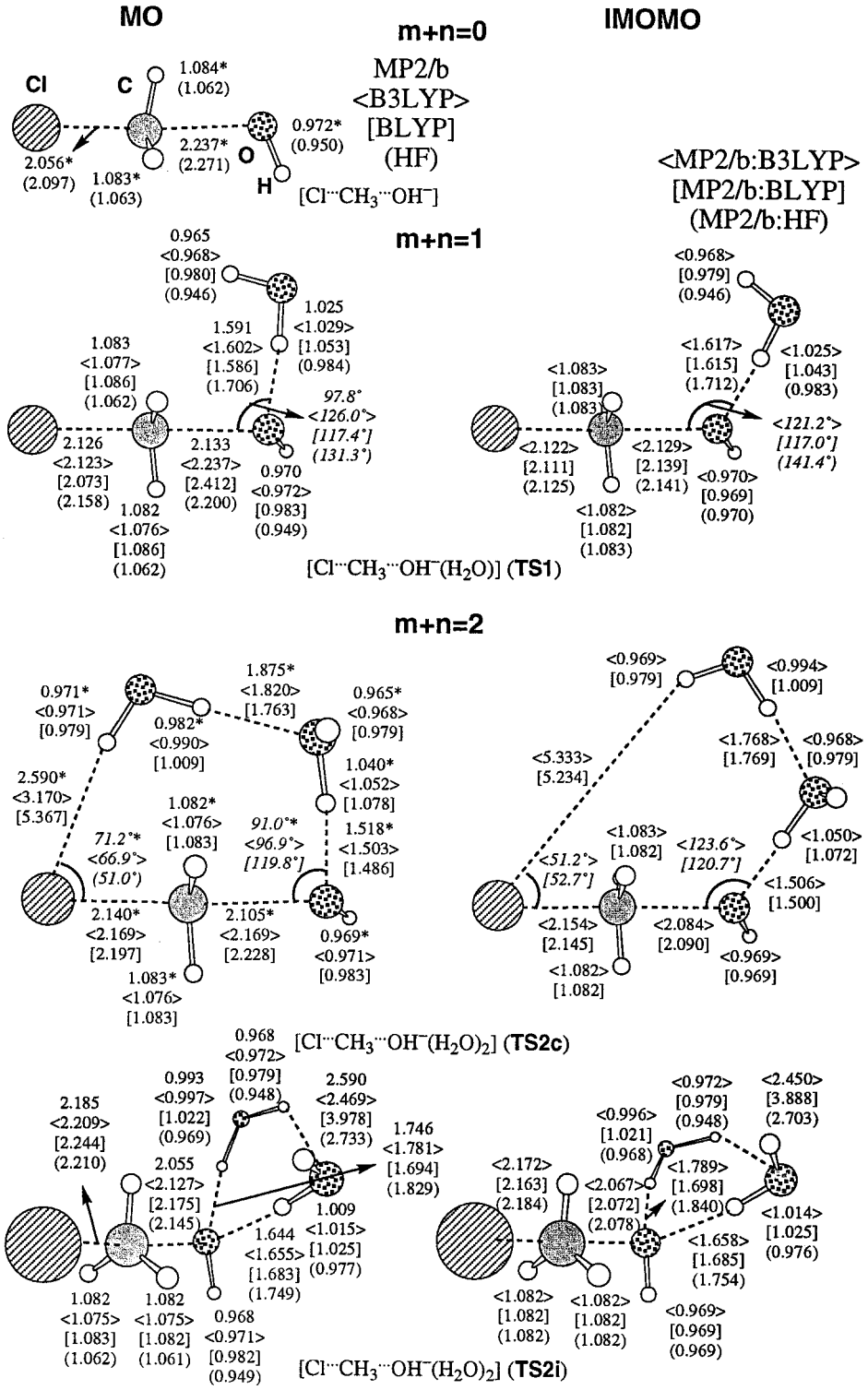

Figure 5. MO and ONIOM optimized geometries (in Å and deg) of transition states for reaction 1 for $m + n = m' + n' = 0$, 1, and 2. For methods used, see Figure 3.

the target MP2/b level. However, the pure BLYP optimization converges to $CH_3Cl(OH^-)$. For the dihydrated system, the three lower pure MO methods including BLYP properly converge the target MP2/b product structure, $CH_2Cl^-(H_2O)_2$. However, geometrical parameters at the pure MO methods suggest that the negative charge is more localized on the Cl part at the MP2/b and B3LYP level but on the CH_2 part at the BLYP. This latter BLYP result is related to the stronger CH_2···HOH interaction, suggested by the unexpectedly short ClH···HOH distance (1.641 Å) and the longer water H−OH bond.

Summarizing, the HF method poorly describes the geometries, (**RC2**) and (**TS2c**), where the solvent molecules bound on the solute part very weekly. The DFT methods could be better candidate as the lower level in the ONIOM method, although they have some significant discrepancy compared to the "target", again (a) missing the reactant complex **RC2** having multidimensional hydrogen bonding and (b) differing in the nature of the transition state **TS2c**. In the following section, we will discuss the reliability of the ONIOM method coupled with the DFT as well as HF methods.

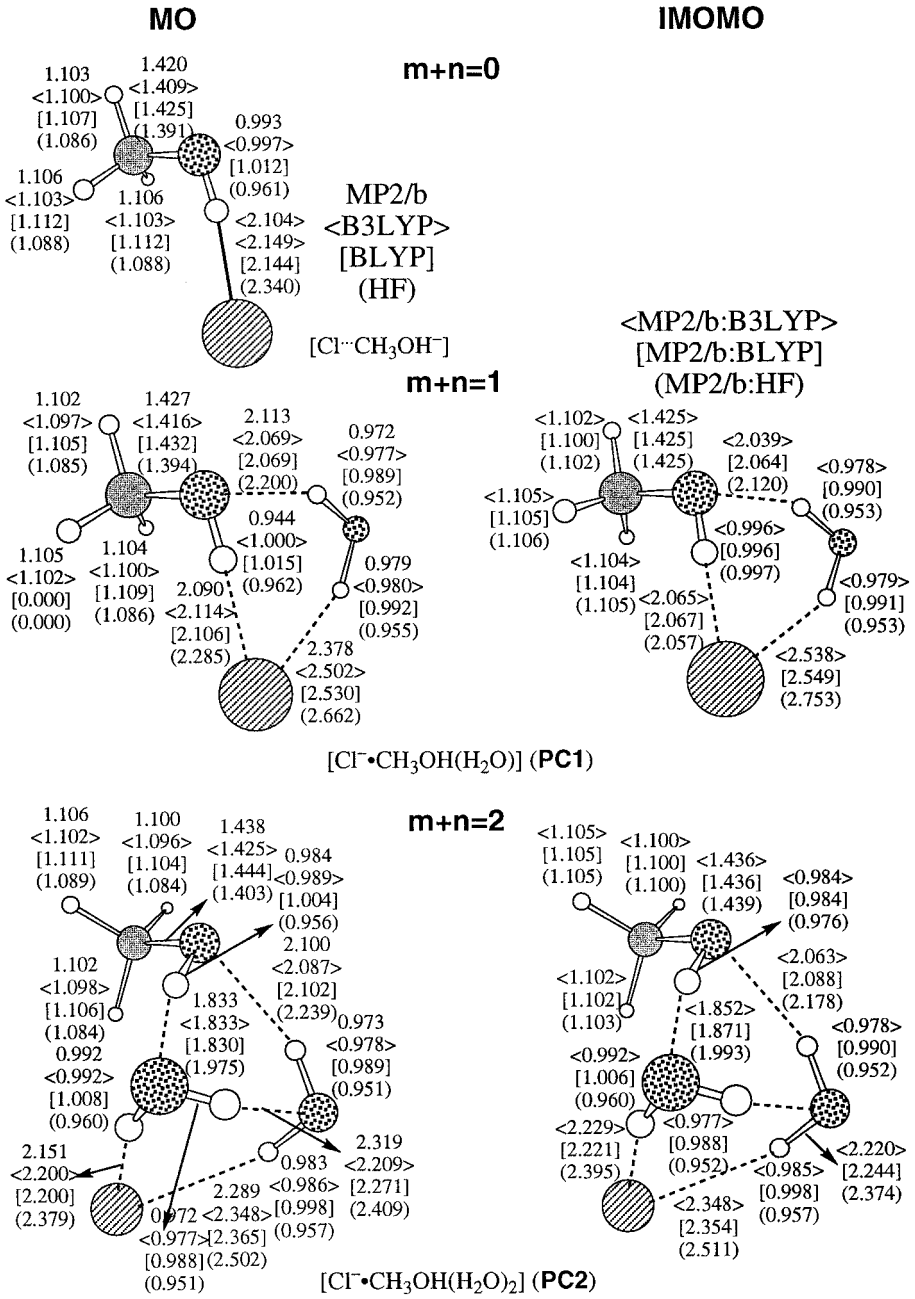

Figure 6. MO and ONIOM optimized geometries (in Å and deg) of product complexes for reaction 1 for $m + n = m' + n' = 0$, 1, and 2. For methods used, see Figure 3.

ONIOM Optimized Geometries. The ONIOM optimized geometries are all shown in the right column of Figures 3−8. Optimized geometries of reactant species in Figure 3 show, as expected, that the structural parameters of OH^-, CH_3Cl, and CH_3OH parts are similar to those at the higher level, MP2/b, and the remaining parts including the intermolecular hydrogen bonds are quite similar to those evaluated with the corresponding lower level methods. We note that in $CH_3Cl(H_2O)_2$ there are substantial differences in $ClCH_3\cdots OH_2$ hydrogen bond distances between the (MP2/b:BLYP) and (MP2/b:HF) methods and the corresponding pure MO methods.

Optimized structures of the reactant complexes with the ONIOM methods are shown in Figure 4. In the (MP2/b:BLYP) level of the ONIOM calculation for the $n + m = 1$ system (**RC1**), the $C\cdots OH^-$ distance is much closer to the higher level value, leading to a significant improvement of the structure. The best ONIOM geometry, compare with the target MP2/b geometry, is obtained at the (MP2/b:B3LYP) level, whereas the hydrogen bond lengths are again found to be poor at the (MP2/b:BLYP) level as in the case of reactants. For the dihydrated system (**RC2**), the ONIOM method both at (MP2/b:B3LYP) and (MP2/b:BLYP) levels provide the multiring structure, although one hydrogen bonding between water molecules is very much weakened. The erroneous situation (a), discussed above, at the pure MO level is thus successfully improved in the ONIOM calculations. This implies that the $ClCH_3\cdots OH^-$ interaction is important in describing correctly the overall structure of the hydrated system. Note that ONIOM (MP2/b:HF) calculation gave only the singly hydrogen bonded structure (**RC2′**). It is therefore obvious that the electron correlation must be included into the lower level of calculation in order to correctly describe the weakly bounded complex **RC2**.

Figure 5 depicts the ONIOM optimized geometries of the transition state for the hydrated ($n + m = 1$ and 2) systems.

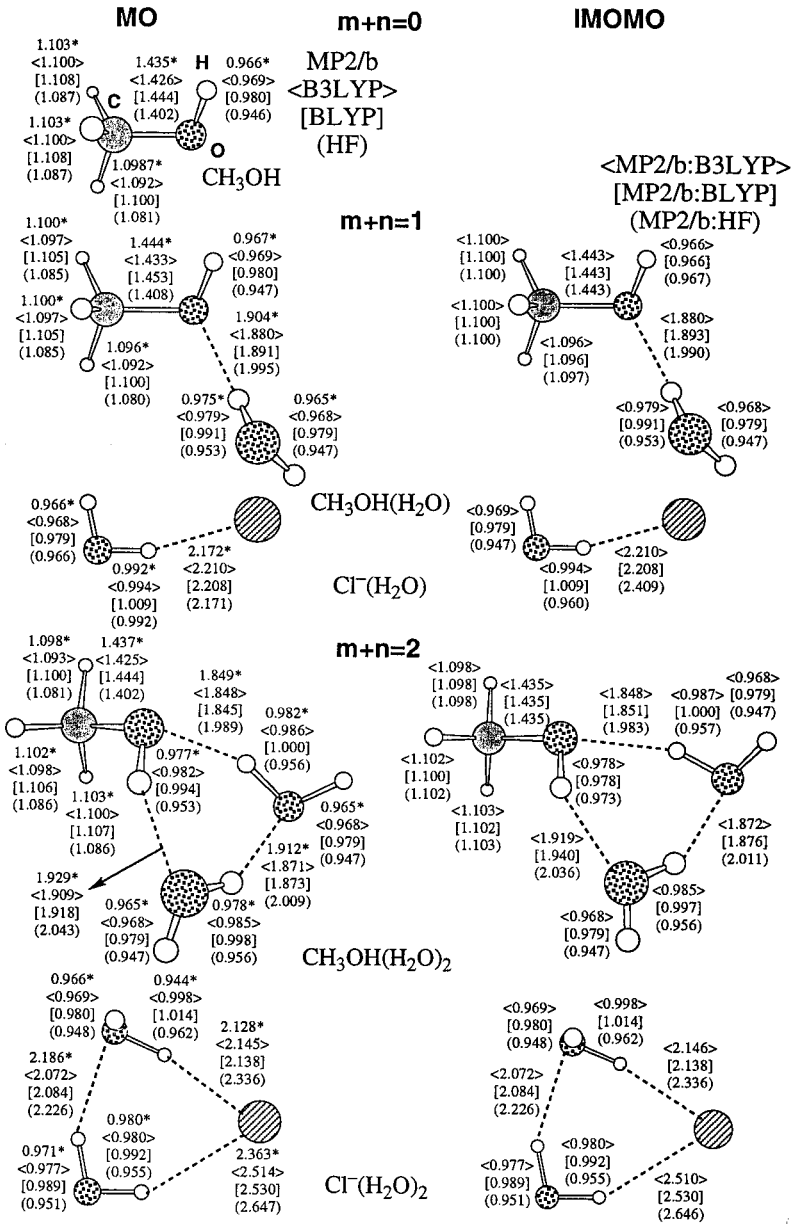

Figure 7. MO and ONIOM optimized geometries (in Å and deg) of product species for reaction 1 for $m + n = m' + n' = 0$, 1, and 2. For methods used, see Figure 3.

Although the higher MP2/b treatment on the active part in the ONIOM calculation does not improve the large ∠C−O−H angle in **TS1**, the geometry of the active part C···CH_3···OH^- becomes much closer to the MP2/b result. For the hydrated system ($n + m = 2$), the erroneous situation (b) is again significantly improved by the ONIOM calculation. The Cl−C bond is longer than that of Cl−O at the (MP2/b:DFT) level, consistent with the "target" result. Although the Cl···HOH distance is calculated to be ca. 5 Å and two water molecules are closer to OH^- at the (MP2/b:DFT) level as compared to the "target", the ONIOM transition states still have the concerted feature. On the other hand, as is anticipated from the pure HF results, **TS2c** could not be obtained at the (MP2/b:HF) level.

Figure 6 illustrates the ONIOM optimized geometries of the product complexes for the mono- (**PC1**) and dihydrated systems (**PC2**). For the product complexes, all of the ONIOM methods reasonably reproduce the target MP2/b geometries. The ONIOM optimized geometries for the product species for the S_N2 channel are also in reasonable agreement with the "target" geometries as shown in Figure 7. However, there exist some discrepancies between the ONIOM and "target" results for the hydrogen abstraction channel. For the monohydrated system, the ONIOM (MP2/b:B3LYP) and (MP2/b:HF) calculations give similar structures to that of the "target", whereas the ONIOM (MP2/b:BLYP) method does not, with optimizations converging to $CH_3Cl(OH^-)$. Similarly, this method is unable to locate the $CH_2Cl^-(H_2O)_2$ structure for the dihydrated system. This is understandable from the strong CH_2···HOH interaction at the pure BLYP result as discussed in the previous section.

Summarizing the findings in the present section, one can conclude that the ONIOM coupled with the B3LYP methods as the lower level could be a good approximation of the target MP2/b geometries for the reaction between $(H_2O)_nCH_3Cl$ and $OH^-(H_2O)_m$ ($n + m = 1$ and 2). On the other hand, the (MP2/b:BLYP) level of the ONIOM method can be good, in the present case, only for the S_N2 channel but not for the hydrogen abstraction channel. The (MP2/b:HF) is not appropriate to describe the geometries for this reaction, indicating the necessity of correlation treatment not only for the active part but also for the solute−solvent and solvent−solvent interactions.

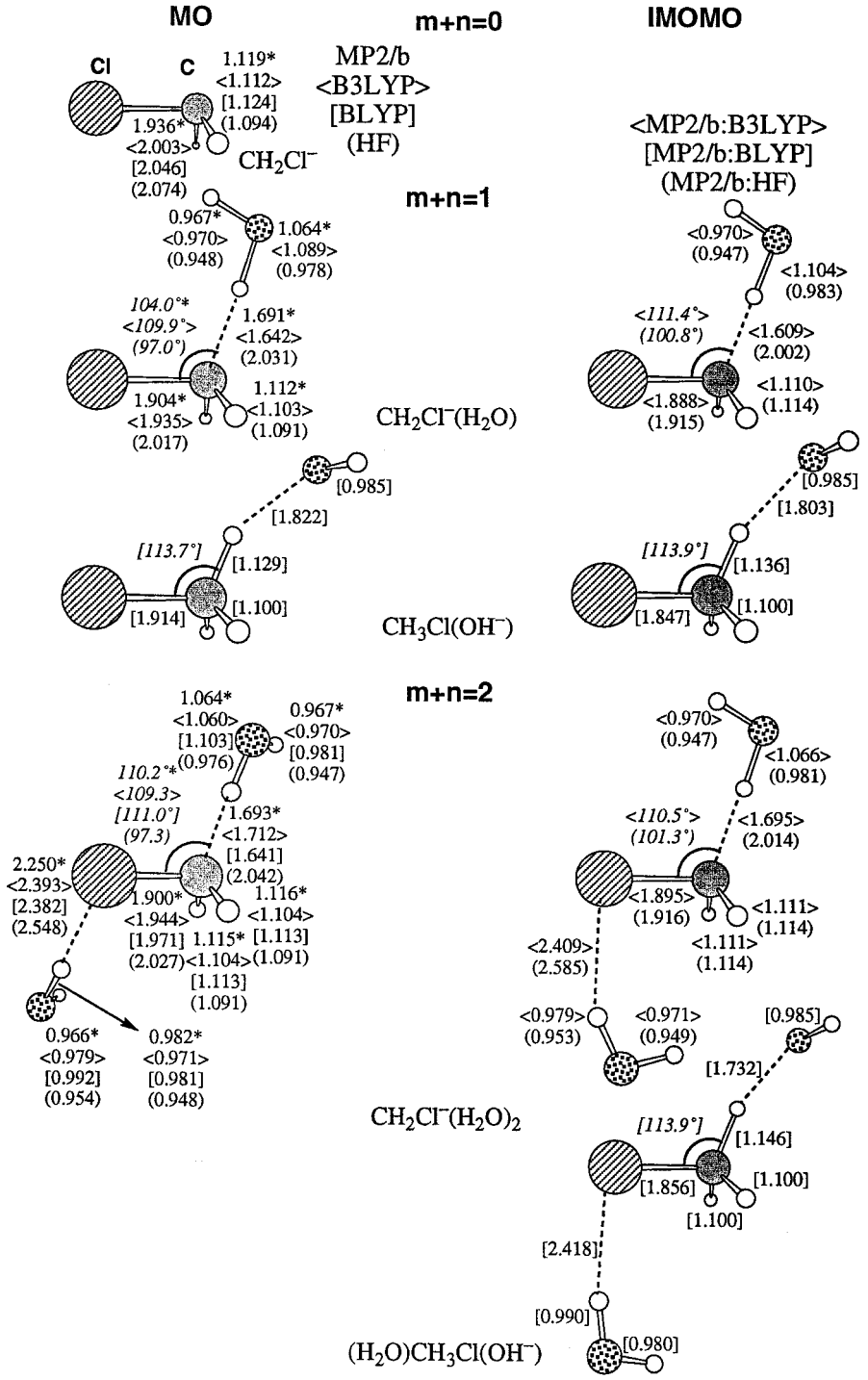

Figure 8. MO and ONIOM optimized geometries (in Å and deg) of product species for the hydride abstraction channel for reaction 2 for $m + n = m' + n' = 0$, 1, and 2. For methods used, see Figure 3.

B. MO and ONIOM Energies. *HF and DFT vs "Target" (MP2/b) Energies.* Table 1 summarizes the energetics for the reaction obtained with the various pure MO and ONIOM methods at the respectively optimized geometries. For the $n + m = 1$ system, at the "target" (MP2/b) level, the reactant complex (**RC1**) is stabilized from the most stable reactant, $OH^-(H_2O) + CH_3Cl$, by 14.3 kcal/mol, which climbs the barrier of 7.2 kcal/mol before reaching very exothermically the product complex. In comparison with the "target" values, the three other pure MO methods generally underestimate the stabilization energy of the reactant complex (**RC1**) as well as the activation barrier from **RC1** to **TS1**. For instance, the B3LYP method underestimates the stabilization energy of **RC1** by 1.6 kcal/mol and the activation barrier by as much as 4.8 kcal/mol. Note that a large overestimation is found for the stability of the product complex (**PC1**) as well as various product species at the HF level. The average absolute errors are 2.7, 2.8, and 7.4 kcal/mol for the B3LYP, BLYP, and HF methods.

ONIOM Energies. The successful integration in the ONIOM method is found for the (MP2/b:HF) level for which the absolute averaged error is very much reduced to 0.9 kcal/mol, clearly an acceptable error. On the other hand, the error at the (MP2/b:B3LYP) level is reduced only a little, and that at the (MP2/b:BLYP) level is even increased. Most of the improvement in

TABLE 1: Calculated Relative Energies (in kcal/mol) of the Reactions 1 and 3 with $m + n = 0$, 1, and 2 Obtained at Various Pure MO and ONIOM Levels at the Respectively Optimized Geometries[a]

		MO[b] MP2/b[c]	IMOMO (MP2/b:B3LYP)	MO B3LYP	IMOMO (MP2/b:BLYP)	MO BLYP	IMOMO (MP2/b:HF)	MO HF
				$m + n = 0$				
$OH^- + CH_3Cl$		0.0						
$[CH_3Cl\cdots OH^-]$	**RC0**	−16.4						
$[Cl^-\cdots CH_3\cdots OH]^-$	**TS0**	−13.4						
$[Cl^-\cdots CH_3OH]$	**PC0**	−						
$Cl^- + CH_3OH$		−51.7						
				$m + n = 1$				
$OH^- + CH_3Cl\cdot(H_2O)$		22.4	26.5 (4.1)	26.5 (4.1)	27.1 (4.7)	26.9 (4.5)	22.3 (0.1)	22.4 (0.0)
$OH^-\cdot(H_2O) + CH_3Cl$		0.0	0.0	0.0	0.0	0.0	0.0	0.0
$[CH_3Cl\cdots OH^-]\cdot H_2O$	**RC1**	−14.3	−12.8 (1.5)	−12.7 (1.6)	−12.3 (2.0)	−12.8 (1.5)	−13.3 (1.0)	−12.7 (1.6)
$[Cl^-\cdots CH_3\cdots OH]^-\cdot H_2O$	**TS1**	−7.1	−5.4 (1.7)	−10.3 (−3.2)	−4.6 (2.5)	−12.4 (−5.3)	−8.6 (−1.5)	−7.5 (−0.4)
$[Cl^-\cdots CH_3OH]\cdot H_2O$	**PC1**	−56.7	−53.4 (3.3)	−57.9 (−1.2)	−52.7 (4.0)	−53.6 (3.1)	−56.3 (0.4)	−69.3 (−12.6)
$H_2O + CH_2Cl^-\cdot(H_2O)$		15.8	16.5 (0.7)	18.0 (2.2)	9.5 (6.3)	12.0 (3.8)	17.7 (1.9)	13.5 (2.3)
$Cl^- + CH_3OH\cdot(H_2O)$		−31.2	−28.7 (2.5)	−34.6 (−3.4)	−28.2 (3.0)	−30.6 (0.6)	−32.4 (−1.2)	−49.6 (−18.4)
$Cl^-\cdot(H_2O) + CH_3OH$		−39.7	−37.0 (2.7)	−42.9 (−3.2)	−36.8 (2.9)	−39.2 (0.5)	−39.4 (0.3)	−56.7 (−17.0)
averaged absolute error			(2.4)	(2.7)	(3.6)	(2.8)	(0.9)	(7.4)
				$m + n = 2$				
$OH^- + CH_3Cl\cdot(H_2O)_2$		40.5	48.0 (7.5)		48.4 (7.9)		42.0 (1.5)	
$OH^-\cdot(H_2O) + CH_3Cl\cdot(H_2O)$		17.7	21.1 (3.4)		20.9 (3.2)		19.4 (1.7)	
$OH^-\cdot(H_2O)_2 + CH_3Cl$		0.0	0.0		0.0		0.0	
$[CH_3Cl\cdots OH^-]\cdot 2H_2O$	**RC2**	−12.6	−10.4 (2.2)		−9.7 (2.9)		−11.1 (1.5)	
$[Cl^-\cdots CH_3\cdots OH]^-\cdot 2H_2O$	**TS2c**	−0.2	4.1 (4.3)		4.6 (4.8)		NA	
$[Cl^-\cdots CH_3\cdots OH]^-\cdot 2H_2O$	**TS2s**	−1.9	1.1 (3.0)		2.0 (3.9)		1.1 (3.0)	
$[Cl^-\cdots CH_3OH]\cdot 2H_2O$	**PC2**	−48.0	−42.1 (5.9)		−41.2 (6.8)		−42.6 (5.4)	
$H_2O + CH_2Cl^-\cdot(H_2O)_2$		29.0	30.8 (1.8)		26.1 (2.9)		30.6 (1.6)	
$Cl^- + CH_3OH\cdot(H_2O)_2$		−20.2	−16.9 (3.3)		−16.2 (4.0)		−20.2 (0.0)	
$Cl^-\cdot(H_2O) + CH_3OH\cdot(H_2O)$		−23.9	−19.5 (4.4)		−19.4 (4.5)		−22.9 (1.0)	
$Cl^-\cdot(H_2O)_2 + CH_3OH$		−32.8	−28.0 (4.8)		−27.9 (4.9)		−30.2 (2.6)	
averaged absolute error			(4.0)		(4.6)		(2.0)	

[a] The numbers in parentheses are the differences from the target MP2/b calculation. [b] Target calculation. [c] MP2/b = MP2/aug−cc-pVDZ; B3LYP = B3LYP/6-31+G(d); BLYP = BLYP/6-31+G(d); HF = HF/6-31+G(d).

the (MP2/b:HF) level comes from the relative energies of **PC1** and various product species. Although the (MP2/b:HF) level of the ONIOM method gives a much better average performance than (MP2/b:DFT), the latter gives much better barrier heights than the former. For example, the barrier at the (MP2/b:B3LYP) level is 7.4 kcal/mol vs 7.2 kcal/mol at the "target" MP2/b, whereas (MP2/b:HF) for the energy barrier in comparison with 4.7 kcal/mol at the level.

For the $n + m = 2$ system, the energy barriers from the reactant complex (**RC2**) to transition states **TS2c** and **TS2s** are obtained to be 12.4 and 10.7 kcal/mol, respectively, at the "target" calculation. The transition state **TS2s** for the substitution/CH_3 inversion followed by the migration of H_2O molecules from the OH^- side to between Cl^- and $HO-CH_3$ is slightly more favorable than the concerted transition state **TS2c**. The relative energies of "concerted" and "stepwise" transition state are correctly reproduced at the ONIOM (MP2/b:DFT) level of the calculations. For instance, the two barrier heights are 14.5 and 11.5 kcal/mol at the (MP2/b:B3LYP). In contrast, we are not able to discuss such a relationship because, as discussed in the previous section, (MP2/b:HF) level totally misses **TS2c**, although the averaged absolute error of 2.0 kcal/mol is again much better than those for the (MP2/b:DFT).

Summarizing this section, the average error of the ONIOM (MP2/b:HF) method is pretty small, but this combination misses a transition state because of the poor performance of the HF method in transition state optimization. On the other hand, the ONIOM (MP2:DFT) methods give large averaged absolute error but reproduce the barriers at transition states quite well.

Improvement of Energies. As discussed above, Garrett and Borisov found that CC/b//MP2/b calculation, i.e., geometry optimization at the MP2/aug-cc-pVDZ level and the improved single energy calculation at the CCSD(T)/aug-cc-pVDZ level, reproduces the experimental results quantitatively. Obviously this is our target calculation. In Table 2, we summarize the energetics of the reaction improved at various levels of single-point calculations at the (MP2/b:DFT) geometries and compare with the "target" (CC/b) results. The CC/b calculation at the (MP2/b:B3LYP) or (MP2/b:BLYP) geometries quantitatively reproduces the target CC/b//MP2/b values with an average absolute error of 0.6 kcal/mol or less for both $n + m = 1$ and 2 systems, indicating that the ONIOM (MP2/b:DFT) geometries are quite reliable, and does not cause significant error in the energetics. Because the (MP2/b:DFT) geometries for **TS2c** are slightly different from the target MP2/b geometry as shown in Figure 5, the relatively large errors (2.2 kcal/mol) are found for **TS2c** at both the CC/b//(MP2/b:B3LYP) and CC/b//(MP2/b:BLYP) levels. Note that the wrong product structure of the proton-transfer reaction at the (MP2/b:BLYP) level results in a large error (−3.8 kcal/mol) at the CC/b//(MP2/b:BLYP) level.

For both monohydrated ($n + m = 1$) and dihydrated ($n + m = 2$) systems, the ONIOM energetics at the geometries determined at the (MP2/b:B3LYP) are on the average slightly more favorable than those at the (MP2/b:BLYP) geometries. The comparison of the improved energies evaluated at the (CC/b:MP2) and (CC/b:B3LYP) level shows that MP2 is more suitable than B3LYP as a lower level when combined with the CC/b level. The absolute averaged errors at the (CC/b:MP2) level are found to be 0.6 and 1.5 kcal/mol for mono- and dihydrated systems, respectively, well within usual experimental errors of thermal measurements. Table 2 also shows that the barrier heights for reaction 1 are obtained with errors of −1.1,

TABLE 2: Calculated Relative Energies (in kcal/mol) of the Reactions 1 and 3 with $m + n = 0$, 1, and 2 Obtained at Various Pure MO and ONIOM Levels at the Respectively Optimized Geometries[a]

energy geometry		MO[b] CC/b[c] MP2/b	IMOMO(MP2/b:B3LYP) MO CC/b	IMOMO(MP2/b:B3LYP) IMOMO (CC/b:MP2)	IMOMO(MP2/b:B3LYP) IMOMO (CC/b:B3LYP)	IMOMO(MP2/b:BLYP) MO CC/b	IMOMO(MP2/b:BLYP) IMOMO (CC/b:MP2)	IMOMO(MP2/b:BLYP) IMOMO (CC/b:BLYP)
				$n = 0$				
$OH^- + CH_3Cl$		0.0						
$[CH_3Cl\cdots OH^-]$		−16.9						
$[Cl^-\cdots CH_3\cdots OH]^-$		−15.3						
$[Cl^-\cdots CH_3OH]$		−						
$Cl^- + CH_3OH$		−53.6						
				$m + n = 1$				
$OH^- + CH_3Cl\cdot(H_2O)$		22.6	22.6 (0.0)	23.6 (1.0)	26.4 (3.8)	22.4 (−0.2)	23.4 (0.8)	27.0 (4.4)
$OH^-\cdot(H_2O) + CH_3Cl$		0.0	0.0	0.0	0.0	0.0	0.0	0.0
$[CH_3Cl\cdots OH^-]\cdot H_2O$	**RC1**	−14.7	−14.7 (0.0)	−14.3 (0.4)	−13.2 (1.5)	−14.6 (0.1)	−14.2 (0.5)	−12.7 (2.0)
$[Cl^-\cdots CH_3\cdots OH]^-\cdot H_2O$	**TS1**	−9.1	−8.9 (0.2)	−9.8 (−0.7)	−7.4 (1.7)	−9.0 (0.1)	−10.0 (−0.9)	−6.6 (2.5)
$[Cl^-\cdots CH_3OH]\cdot H_2O$	**PC1**	−58.4	−58.2 (0.2)	−58.6 (−0.2)	−55.2 (3.2)	−58.4 (0.0)	−58.8 (−0.4)	−54.5 (3.9)
$H_2O + CH_2Cl^-\cdot(H_2O)$		13.6	14.0 (0.4)	12.2 (1.4)	13.5 (−0.1)	9.8 (−3.8)	4.0 (−9.6)	7.0 (−6.6)
$Cl^- + CH_3OH\cdot(H_2O)$		−32.9	−32.9 (0.0)	−33.3 (−0.4)	−30.7 (2.2)	−33.1 (−0.2)	−33.6 (−0.7)	−30.2 (2.7)
$Cl^-\cdot(H_2O) + CH_3OH$		−41.4	−41.4 (0.0)	−41.2 (0.2)	−39.0 (2.4)	−41.6 (−0.2)	−41.4 (0.0)	−38.7 (2.7)
averaged absolute error			(0.1)	(0.6)	(2.2)	(0.6)	(1.8)	(3.6)
				$m + n = 2$				
$OH^- + CH_3Cl\cdot(H_2O)_2$		40.7	40.8 (0.1)	44.4 (3.7)	47.9 (7.2)	40.8 (0.1)	44.1 (3.4)	48.3 (7.6)
$OH^-\cdot(H_2O) + CH_3Cl\cdot(H_2O)$		17.8	17.9 (0.1)	20.4 (2.6)	21.0 (3.2)	18.0 (0.2)	20.3 (2.5)	20.9 (3.1)
$OH^-\cdot(H_2O)_2 + CH_3Cl$		0.0	0.0	0.0	0.0	0.0	0.0	0.0
$[CH_3Cl\cdots OH^-]\cdot 2H_2O$	**RC2**	−13.1	−13.5 (−0.4)	−12.1 (1.0)	−10.7 (2.4)	−13.3 (−0.2)	−12.0 (1.1)	−10.0 (3.1)
$[Cl^-\cdots CH_3\cdots OH]^-\cdot 2H_2O$	**TS2c**	−2.1	0.1 (2.2)	−0.4 (1.7)	1.9 (4.0)	0.1 (2.2)	−0.6 (1.5)	2.5 (4.6)
$[Cl^-\cdots CH_3\cdots OH]^-\cdot 2H_2O$	**TS2s**	−4.0	−3.8 (0.2)	−4.4 (−0.4)	−1.1 (2.9)	−3.7 (0.3)	−4.1 (−0.1)	−0.2 (3.8)
$[Cl^-\cdots CH_3OH]\cdot 2H_2O$	**PC2**	−49.9	−49.6 (0.3)	−48.6 (1.3)	−44.2 (5.7)	−49.7 (0.2)	−48.8 (1.1)	−43.3 (6.6)
$H_2O + CH_2Cl^-\cdot(H_2O)_2$		26.9	24.8 (−2.1)	25.8 −(1.1)	29.7 (2.8)	24.5 (−2.4)	21.2 (−5.7)	23.5 (−3.4)
$Cl^- + CH_3OH\cdot(H_2O)_2$		−21.8	−21.6 (0.2)	−21.9 (−0.1)	−18.9 (2.9)	−21.8 (0.0)	−22.2 (−0.4)	−18.2 3.6)
$Cl^-\cdot(H_2O) + CH_3OH\cdot(H_2O)$		−25.4	−25.3 (0.1)	−24.1 (1.3)	−21.4 (4.0)	−25.4 (0.0)	−22.4 (1.0)	−21.4 (4.0)
$Cl^-\cdot(H_2O)_2 + CH_3OH$		−34.5	−34.3 (0.2)	−32.7 (1.8)	−29.9 (4.6)	−34.4 (0.1)	−32.9 (1.6)	−29.8 4.7)
averaged absolute error			(0.6)	(1.5)	(4.0)	(0.6)	(1.9)	(4.4)

[a] The numbers in parentheses are the differences from the target CC/b//MP2/b calculation. [b] The target calculation. [c] CC = CCSD(T)/aug-cc-pVDZ; MP2/b = MP2/aug-cc-pVDZ; MP2 = MP2/6-31+G(d); B3LYP = B3LYP/6-31+G(d).

+0.7, and −1.4 kcal/mol for **RC1 → TS1** (for $m + n = 1$), **RC2 → TS2c**, and **RC2 → TS2s** (both for $m + n = 2$) with the ONIOM (CC/b:MP2) method at the ONIOM (MP2/b:B3LYP) geometries, compared with the "target" values of 5.6, 11.0, and 9.1 kcal/mol. With the ONIOM (CC/b:B3LYP) method at the ONIOM (MP2/b:B3LYP) geometries, the corresponding errors are +0.2, +1.6, and +0.5 kcal/mol.

One notices in both ONIOM (CC/b:MP2)//(MP2/b:B3LYP) and ONIOM (CC/b:MP2)//(MP2/b:B3LYP) methods that the error increased with the number of low level water molecules: 0.6−1.5 kcal/mol for $m + n = 1-2$ for the former method and 2.2−4.4 kcal/mol for the latter. This is in a sense as expected, because the error mainly comes from the interaction of the low level water molecules with the solute, which should increase with the number of water molecules.

Consequently, we can say that the ONIOM (CC/b:MP2)//(MP2/b:B3LYP) method is the best candidate among the ONIOM methods we tested. At this level, we can obtain an excellent approximation for the geometry and energetics (<1.0 kcal/mol error per solvent water molecule) of the reaction 1 potential energy surface at the CC/b//MP2/b level of theory which is too expensive to perform. The ONIOM (CC/b:B3LYP)//(MP2/b:B3LYP) method is also a possible choice, if one can tolerate a larger error (∼2.0 kcal/mol error per solvent water molecule).

C. Selection of the Lower Level Method. *S-Value Tests with MP2/b as the High Level.* The accuracy of the ONIOM energetics depends much on the lower level of the method used. Thus, the selection of the lower level is critically important for the success of the ONIOM calculation as shown in above section. The S-value test is a systematic way of evaluating the performance of low level methods against the "target" high level. In the ONIOM method, the target high level energy of the real system, E(high, real) is approximated by E(ONIOM, real) defined by eq 2. Therefore, the error introduced by using E(ONIOM, real) instead of E(real, high) is defined as[33]

$$\begin{aligned}\delta &= E(\text{high, real}) - E(\text{ONIOM, real})\\ &= [E(\text{high, real}) - E(\text{high, model})] - \\ &\qquad [E(\text{low, real}) - E(\text{low, model})]\\ &= S(\text{high}) - S(\text{low}) \qquad (4)\end{aligned}$$

The quantities in the square brackets in the second equation of eq 4, represent the difference between the real system and model system, evaluated high and low level, respectively, and are called the substituent effects or S value at each level, S(high) and S(low). Equation 4 shows that the ONIOM energy will match exactly the target E(high, real) if S(low) is equal to S(high). When one wants to use the ONIOM method, one does not know S(high), because this requires E(high, real) results which one wants to avoid calculating. However, in the present study, we have the target E(high, real) and therefore S(high) for all of the systems under study. Therefore, we will compare S(high) with various levels of S(low). The low level that gives the smallest absolute error of S(low) from S(high) is the best low level method to be used with this high level.

In Table 3, for all of the reactants, reactant complexes, transition states, product complexes, and products, we compare the S value (relative to the reference reactants of $OH^-(H_2O)_{n+m}$

TABLE 3: *S* values, *S*(level) = [*E*(level, real) − *E*(level, model)] (in kcal/mol, Relative to the Reactants $OH^-(H_2O)_{m+n}$ + CH_3Cl), Evaluated at the MP2/b (High Level) and Various Lower Level MO Methods for the Reactions 1 and 3 with $m + n = 1$ and 2[a]

method		S(high) MP2/b[b]	*S*(low) B3LYP	BLYP	HF
		$n + m = 1$			
$OH^- + CH_3Cl(H_2O)$		22.4	26.5 (4.1)	26.9 (−4.5)	21.5 (0.9)
$OH^-(H_2O) + CH_3Cl$		0.0	0.0 (0.0)	0.0 (0.0)	0.0 (0.0)
$[CH_3Cl\cdots OH^-]\cdot H_2O$	**RC1**	1.1	2.7 (−1.5)	3.3 (−2.1)	2.5 (−1.4)
$[Cl^-\cdots CH_3\cdots OH]^-\cdot H_2O$	**TS1**	7.0	9.1 (−2.1)	9.8 (−2.8)	6.3 (0.7)
$[Cl^-\cdots CH_3OH]\cdot H_2O$	**PC1**	11.0	14.5 (−3.5)	15.1 (−4.1)	11.3 (−0.3)
$H_2O + CH_2Cl^-(H_2O)$		4.6	5.5 (−0.9)	5.1 (−0.5)	7.3 (−2.7)
$Cl^- + CH_3OH(H_2O)$		20.5	23.2 (−2.7)	23.6(−3.1)	18.6 (1.9)
$Cl^-(H_2O) + CH_3OH$		12.0	14.7 (−2.6)	14.7 (−2.7)	11.9 (0.1)
averaged absolute error			(2.5)	(2.9)	(1.1)
		$n + m = 2$			
$OH^- + CH_3Cl(H_2O)_2$		40.4	48.0 (−7.6)	48.3 (−7.9)	41.5 (−1.1)
$OH^-(H_2O) + CH_3Cl(H_2O)$		17.7	21.1 (−3.4)	21.0 (−3.3)	19.8 (−2.1)
$OH^-(H_2O)_2 + CH_3Cl$		0.0	0.0 (0.0)	0.0 (0.0)	0.0 (0.0)
$[CH_3Cl\cdots OH^-]\cdot 2H_2O$	**RC2**	2.2	5.7 (−3.5)	6.5 (−4.2)	5.6 (−3.4)
$[Cl\cdots CH_3\cdots OH]^-\cdot 2H_2O$	**TS2c**	14.2	19.4 (−5.1)	20.2 (−6.0)	17.3 (−3.1)
$[Cl\cdots CH_3\cdots OH]^-\cdot 2H_2O$	**TS2s**	13.9	17.1 (−3.2)	18.0 (−4.1)	
$[Cl^-\cdots CH_3OH]\cdot 2H_2O$	**PC2**	11.8	18.1 (−6.2)	18.8 (−7.0)	18.5 (−6.7)
$H_2O + CH_2Cl^-(H_2O)_2$		17.8	21.5 (−3.7)	20.5 (−2.7)	23.5 (−5.7)
$Cl^- + CH_3OH(H_2O)_2$		31.4	35.0 (−3.5)	35.5 (−4.0)	31.1 (0.3)
$Cl^-(H_2O) + CH_3OH(H_2O)$		27.8	32.4 (−4.7)	32.4(−4.6)	28.8 (−1.1)
$Cl^-(H_2O)_2 + CH_3OH$		18.9	23.8 (−4.9)	23.8(−4.9)	21.8 (−2.9)
averaged absolute error			(4.6)	(4.9)	(2.9)

[a] All calculations are performed at the geometries determined at the MP2/aug-cc-pVDZ (MP2/b) level. The numbers in parentheses are values of $\delta = S(\text{high}) - S(\text{low})$. [b] Reference 15 and present work.

+ CH_3Cl) at the target MP2/b level with those at the B3LYP, BLYP, and HF levels. All of the *S* values were calculated at the MP2/b optimized geometries. The average absolute error in the *S* value is 2.5, 2.9, and 1.1 kcal/mol for B3LYP, BLYP, and HF method, respectively, for the monohydrated ($n + m = 1$) system and 4.6, 4.9, and 2.9 kcal/mol, respectively, for the dihydrated ($n + m = 2$) system. This suggests that in the ONIOM method where the high level is MP2/b, HF does better than B3LYP and BLYP as the lower level. This may sound surprising, because B3LYP and BLYP somehow have taken the electron correlation into account, whereas HF does not. We have encountered a similar situation before in the ONIOM calculation of C═C bond dissociation energy.[17b] We believe that the errors in the HF method is systematic, and the effect of the low level solvent molecules on the energetics is reasonably reproduced. On the other hand, the errors in the density functional methods are random because of the semiempirical nature of parametrization and the effects of the low level solvent molecules also contain the same random error.

S-Value Tests with CC/b as the High Level. We performed a similar *S*-value test at (MP2/b:B3LYP) geometries adopting CC/b as the high level and MP2 and B3LYP as low levels, as shown in Table 4. The average absolute errors of the ONIOM (CC/b:MP2) single-point energies, compared to the CC/b target energies, are 0.8 and 1.4 kcal/mol for the $m + n = 1$ and 2 systems, respectively, and those of (CC/b:B3LYP) are 2.2 and 3.9 kcal/mol, respectively. The errors for the (CC/b:MP2) combination are much smaller than those for (CC/b:B3LYP) and any other ONIOM combinations we have examined.

D. Computational Time Requirements. The largest merit of using the ONIOM method is in saving computational time. One can obtain the results nearly as accurate as the target calculation with a fraction of the cost. In addition, in ONIOM, the cost increase with the increase of the size *N* of the system is determined at the low level and is much less steeper than that of the target calculation, which could be of the order of $N^{4\sim6}$ if a method as accurate as CCSD(T) is used. We have documented timing data for $(CH_3Cl)(H_2O)$ and $(CH_3Cl)(H_2O)_2$ using a PC with an Intel Pentium II CPU, as follows: For the $m + n = 1$ system, the cost of ONIOM geometry optimization is about 20% of the pure MO optimization and the cost of single-point improved energy calculation is about 10% of the pure

TABLE 4: *S* values, *S*(level) = [*E*(level, real) − *E*(level, model)] (in kcal/mol, Relative to the Reactants $OH^-(H_2O)_{m+n}$ + CH_3Cl), Evaluated at the CC/b (High Level) and Various Lower Level MO Methods for the Reactions 1 and 3 with $m + n = 1$ and 2[a]

method		*S*(high) CC/b	*S*(low) MP2	B3LYP
		$m + n = 1$		
$OH^- + CH_3Cl(H_2O)$		22.6	23.6 (−1.0)	26.5 (−3.9)
$OH^-(H_2O) + CH_3Cl$		0.0	0.0 (0.0)	0.0 (0.0)
$[CH_3Cl\cdots OH^-]\cdot H_2O$	**RC1**	1.0	1.4 (−0.4)	2.5 (−1.5)
$[Cl^-\cdots CH_3\cdots OH]^-\cdot H_2O$	**TS1**	7.3	6.3 (1.0)	8.7 (−1.4)
$[Cl^-\cdots CH_3OH]\cdot H_2O$	**PC1**	11.0	10.6 (0.3)	14.0 (−3.1)
$H_2O + CH_2Cl^-(H_2O)$		5.8	3.9 (1.9)	5.2 (0.6)
$Cl^- + CH_3OH(H_2O)$		20.8	20.3 (0.5)	22.9 (−2.2)
$Cl^-(H_2O) + CH_3OH$		12.2	12.5 (−0.2)	14.7 (−2.5)
averaged absolute error			(0.8)	(2.2)
		$m + n = 2$		
$OH^- + CH_3Cl(H_2O)_2$		40.8	44.3 (−3.5)	47.9 (−7.1)
$OH^-(H_2O) + CH_3Cl(H_2O)$		17.9	20.4 (−2.4)	21.0 (−3.1)
$OH^-(H_2O)_2 + CH_3Cl$		0.0	0.0 (0.0)	0.0 (0.0)
$[CH_3Cl\cdots OH^-]\cdot 2H_2O$	**RC2**	1.2	2.6 (−1.4)	3.9 (−2.8)
$[Cl\cdots CH_3\cdots OH]^-\cdot 2H_2O$	**TS2c**	17.1	16.6 (0.5)	18.9 (−1.9)
$[Cl\cdots CH_3\cdots OH]^-\cdot 2H_2O$	**TS2s**	13.7	13.1 (0.6)	16.5 (−2.7)
$[Cl^-\cdots CH_3OH]\cdot 2H_2O$	**PC2**	11.6	12.6 (−1.0)	17.0 (−5.3)
$H_2O + CH_2Cl^-(H_2O)_2$		16.6	17.7 (−1.0)	21.7 (−4.9)
$Cl^- + CH_3OH(H_2O)_2$		31.9	31.6 (0.3)	34.7 (−2.8)
$Cl^-(H_2O) + CH_3OH(H_2O)$		28.4	29.5 (−1.2)	32.2 (−3.8)
$Cl^-(H_2O)_2 + CH_3OH$		19.3	20.9 (−1.6)	23.7 (−4.4)
averaged absolute error			(1.4)	(3.9)

[a] All calculations are performed at the geometries determined at the (MP2/aug-cc-pVDZ:B3LYP/6-31+G(d)) (i.e., (MP2/b:B3LPY)) level. The numbers in parentheses are values of $\delta = S(\text{high}) - S(\text{low})$.

Geometry optimization (per cycle)	
$(CH_3Cl)(H_2O)$	Pure MP2/b = 5544 sec
	ONIOM(MP2/b:B3LYP) = 1178 sec
$(CH_3Cl)(H_2O)_2$	Pure MP2/b = 15782 sec
	ONIOM(MP2/b:B3LYP) = 1602 sec
Single point calculation	
$(CH_3Cl)(H_2O)$	Pure CC/b = 16440 sec
	ONIOM(CC/b:MP2) = 1629 sec
$(CH_3Cl)(H_2O)_2$	Pure CC/b = 104965 sec
	ONIOM(CC/b:MP2) = 1922 sec

MO calculation. For the $m + n = 2$ system, this ratio decreases to 10% and less than 2%, respectively. If B3LYP is used in the single-point calculation instead of MP2, the decrease in the cost ratio will be even more dramatic. These ratios will decrease further with m + n > 2.

IV. Concluding Remarks

We have examined the reliability of the two-layered ONIOM method for the S_N2 reaction pathway between CH_3Cl and OH^- ion in microsolvation clusters with one or two water molecules. Only the solute part, CH_3Cl and OH^-, was treated at a high level of molecular orbital (MO) theory, and all solvent water molecules were treated at a low MO level.

Using the MP2/aug-cc-pVDZ optimized geometries of all of the reactants, reactant complexes, transition states, product complexes, and products as the target geometries, the ONIOM optimized geometries with the MP2/aug-cc-pVDZ as the high level and various ab initio and DFT methods as the low level were compared with the "target" geometries. At least the B3LYP/6-31+G(d) level of method is needed as a lower level to describe the hydrogen-bond system properly. We found that the ONIOM (MP2/aug-cc-pVDZ:B3LYP/6-31+G(d)) can reproduce the "target" (MP2/aug-cc-pVDZ) geometries very well. The other ONIOM methods tested in this study do not satisfactorily reproduce the "target" geometries because of the poor performance of the pure low MO level especially for the weakly bonded complexes.

The energetics was improved by performing the high level single-point OINOM energy calculation at the MP2/aug-cc-pVDZ or ONIOM optimized geometries. Here the ONIOM energies in which the high level was CCSD(T)/aug-cc-pVDZ level with the low level of MP2 as well as DFT methods were compared with the "target" CCSD(T)/aug-cc-pVDZ results. ONIOM energies with MP2/aug-cc-pVDZ as the low level reproduce the "target" energies within an average absolute error of less than 1 kcal/mol per solvent water molecule and more than 2 kcal/mol with DFT methods as the lower level. The computational cost for the recommended ONIOM calculations for the dihydrated system was found to be less than 10% of the target calculations, and this ratio is expected to decrease further as the number of solvent molecules increases.

Therefore, considering the accuracy and the cost, the recommended very accurate method from the present study for chemical reactions in microsolvated cluster is ONIOM (CCSD(T)/aug-cc-pVDZ:MP2/6-31+G(d))//ONIOM(MP2/aug-cc-pVDZ:B3LYP/6-31+G(d)).

Acknowledgment. The authors are grateful to Drs. Bruce Garrett and Yurii Borisov for providing the unpublished results of their ab initio calculations. They are also grateful to Prof. Yoshihiro Osamura for some calculations, discussions, and encouragement. The present research is in part supported by a Grant (CHE-9627775) from the National Science Foundation. S.R. acknowledges a research fellowship from the Japan Society for Promotion of Sciences. The generous support of computing time at the Emerson Center of Emory University is acknowledged. K.M. also acknowledge the computer time made available at the Molecular Science Computing Facility, Environmental Molecular Science Laboratory, Pacific Northwest National Laboratory.

References and Notes

(1) Ohta, K.; Morokuma, K. *J. Am. Chem. Soc*. **1985**, *89*, 5845.
(2) Evanseck, J. D.; Blake, J. F.; Jorgensen, W. L. *J. Am. Chem. Soc*. **1987**, *109*, 2349.
(3) Pliego, J. R., Jr.; Almeida, W. R. D. *J. Phys. Chem*. **1996**, *100*, 12410.
(4) Pliego, J. R., Jr.; Almeida, W. R. D. *Chem. Phys. Lett*. **1996**, *249*, 136.
(5) Marrone, P. A.; Arias, T. A.; Peters, W. A.; Tester, J. W. *J. Phys. Chem. A*. **1998**, *102*, 7013.
(6) Fells, I.; Moelwyn-Hughes, E. A. *J. Chem. Soc*. **1959**, 398.
(7) Hine, J. *J. Am. Chem. Soc*. **1950**, *72*, 2438.
(8) Hine, J.; Dowell, A. M. *J. Am. Chem. Soc*. **1954**, *76*, 2688.
(9) Robinson, E. A. *J. Chem. Soc*. **1961**, 1663.
(10) Henchman, M.; Hierl, P. M.; Paulson, J. F. *J. Am. Chem. Soc*. **1985**, *107*, 2812.
(11) Hierl, P. M.; Paulson, J. F.; Henchman, M. J. *J. Phys. Chem*. **1995**, *99*, 15655.
(12) Miertus, S.; Tomasi, *J. Chem. Phys*. **1982**, *65*, 239.
(13) Miertus, S.; Scrocco, E.; Tomasi, *J. Chem. Phys*. **1981**, *55*, 117.
(14) Jensen, F. *Chem. Phys. Lett*. **1992**, *196*, 368.
(15) Borisov, Y. A.; Garrett, B. C. Private communication. The energies of structures for reactants, products, and stable complexes as well as transition state have been obtained at the CCSD(T)/aug-cc-pVDZ//MP2-(FC)/aug-cc-pVDZ level of calculation for one and two hydrated cluster system, $(H_2O)_nOH^- + CH_3Cl(H_2O)_m$, $n + m = 1$ and 2.
(16) Svensson, M.; Humbel, S.; Froese, R. D. J.; Matsubara, T.; Sieber, S.; Morokuma, K. *J. Phys. Chem*. **1996**, *100*, 19357.
(17) (a) Humbel, S.; Sieber, S.; Morokuma, K. *J. Chem. Phys*. **1996**, *105*, 1959. (b) Svensson, M.; Humbel, S.; Morokuma, K. *J. Chem. Phys*. **1996**, *105*, 3654.
(18) Topol, L. A.; Burt, S. K.; Rashin, A. A. *Chem. Phys. Lett*. **1995**, *247*, 112.
(19) Novoa, J. J.; Soza, C. *J. Phys. Chem*. **1995**, *99*, 15837.
(20) Soliva, R.; Orozco, M.; Luque, F. J. *J. Comput. Chem*. **1997**, *18*, 980.
(21) Gonzalez, L.; Mo, O.; Yanez, M. *J. Comput. Chem*. **1997**, *18*, 1124.
(22) Sirois, S.; Proynov, E. I.; Nguyen, D. T.; Salahub, D. R. *J. Chem. Phys*. **1997**, *107*, 6770.
(23) Jiang, J. C.; Tsai, M.-H. *J. Phys. Chem. A* **1997**, *101*, 1982.
(24) Becke, A. D. *J. Chem. Phys*. **1993**, *98*, 1372; 5648.
(25) Miehlich, B.; Savin, A.; Stoll, H.; Preuss, H. *Chem. Phys. Lett*. **1989**, *157*, 200.
(26) Lee, C.; Yang, W.; Parr, R. G. *Phys. Rev. B* **1988**, *37*, 785.
(27) Frisch, M. J.; Trucks, G. W.; Schlegel, H. B.; Scuseria, G. E.; Robb, M. A.; Cheeseman, J. R.; Zakrzewski, V. G.; Montgomery, J. A., Jr.; Stratmann, R. E.; Burant, J. C.; Dapprich, S.; Millam, J. M.; Daniels, A. D.; Kudin, K. N.; Strain, M. C.; Farkas, O.; Tomasi, J.; Barone, V.; Cossi, M.; Cammi, R.; Mennucci, B.; Pomelli, C.; Adamo, C.; Clifford, S.; Ochterski, J.; Petersson, G. A.; Ayala, P. Y.; Cui, Q.; Morokuma, K.; Malick, D. K.; Rabuck, A. D.; Raghavachari, K.; Foresman, J. B.; Cioslowski, J.; Ortiz, J. V.; Stefanov, B. B.; Liu, G.; Liashenko, A.; Piskorz, P.; Komaromi, I.; Gomperts, R.; Martin, R. L.; Fox, D. J.; Keith, T.; Al-Laham, M. A.; Peng, C. Y.; Nanayakkara, A.; Gonzalez, C.; Challacombe, M.; Gill, P. M. W.; Johnson, B. G.; Chen, W.; Wong, M. W.; Andres, J. L.; Head-Gordon, M.; Replogle, E. S.; Pople, J. A. *Gaussian 98*, revision A.1; Gaussian, Inc.: Pittsburgh, PA, 1998.
(28) Tucker, S. C.; Truhlar, D. G. *J. Am. Chem. Soc*. **1990**, *112*, 3347.
(29) Morokuma, K. *J. Am. Chem. Soc*. **1982**, *104*, 3732.
(30) Chandrasekhar, J.; Smith, S. F.; Jorgensen, W. L. *J. Am. Chem. Soc*. **1985**, *107*, 154; **1984**, *106*, 3049.
(31) Xantheas, S. S. *J. Am. Chem. Soc*. **1995**, *117*, 10373.
(32) Asada, T.; Kato, N.; Kitaura, K. *J. Mol. Struct. (THEOCHEM)* **1999**, *461*−*462*, 493.
(33) Vreven, T.; Morokuma, K. *J. Chem. Phys*. **1999**, *111*, 8799.